

Molecular-dynamics investigation of tracer diffusion in a simple liquid

Fouzia Ould-Kaddour* and Jean-Louis Barrat

Laboratoire de Physique, Ecole Normale Supérieure de Lyon, 69364 Lyon CEDEX 07, France

(Received 17 April 1991)

Extensive molecular-dynamics simulations have been carried out for a model tracer-solvent system made up of 100 solvent molecules and 8 tracer molecules interacting through truncated Lennard-Jones potentials. The influence of the size ratio between solute and solvent, of their mass ratio, and of the solvent viscosity on the diffusivity of a small tracer was investigated. Positive deviations from a Stokes-Einstein behavior are observed, in qualitative agreement with experimental observations. It was also observed that as tracer and solvent become increasingly dissimilar, their respective dynamics become decoupled. We suggest that such decouplings can be interpreted by writing the mobility of the tracer as the sum of two terms, the first one arising from a coupling between tracer dynamics and hydrodynamic modes of the solvent, and the second one describing jump motion in a locally nearly frozen environment.

PACS number(s): 66.10.Cb, 02.60.+y

I. INTRODUCTION

It is well known that the diffusion coefficient D of a large and massive particle or molecule (tracer) immersed in a solvent of much smaller and lighter molecules is related to the solvent viscosity η by the Stokes-Einstein (SE) equation

$$D = \frac{k_B T}{6\pi\eta\sigma}, \quad (1)$$

where T is the absolute temperature, k_B the Boltzmann constant, and σ the radius of the diffusing particle. This relation has been verified experimentally in great detail [1] and is theoretically well understood [2].

If, however, the size of the diffusing particle is not large compared to that of the solvent molecule, the Stokes-Einstein relation is not expected to remain valid. Surprisingly, it turns out that the borderline case of self-diffusion in simple liquids (i.e., the case of a tracer particle identical to the solvent molecules) is still well described by Eq. (1) [3]. When, on the other hand, the tracer becomes smaller than the solvent molecules, a large body of experimental evidence shows that (1) is violated [4–7]. Experimental data were often fitted to the modified Stokes-Einstein form:

$$D \sim \eta^{-\alpha}, \quad (2)$$

where the exponent α is smaller than 1. For example, the diffusion coefficient of xenon in a series of n -alkanes was found to obey (2) with $\alpha=0.686$ [6]. The interpretation of such experiments, however, is complicated by the fact that changing one of the two elements of the tracer-solvent combination implies that one simultaneously modifies all the microscopic parameters characterizing this combination; for example, the size ratio of the two molecules, their mass ratio, and their van der Waals interactions are changed at the same time. Each of these parameters can be expected to affect the tracer diffusivity in its own way, and experiments do not have the ability to

sort out these different contributions.

Molecular-dynamics (MD) simulations, on the other hand, allow a continuous variation of the parameters characterizing the solute-solvent system and thus a systematic investigation of the way each of them affects the diffusivity of the tracer. In this paper we present such a systematic investigation of a model system, in which both solvent and solute interact through truncated Lennard-Jones (LJ) potentials. A rather large number of parameters is required to describe even such a simple system, and a systematic exploration of this multidimensional parameter space is clearly out of the question. Therefore, we have chosen to focus on several “cuts” in this parameter space, in order to assess the separate influence of the mass ratio m_2/m_1 (the indices 1 and 2 refer, respectively, to the solvent and solute molecules), of the size ratio σ_2/σ_1 , and of the solvent viscosity, all other parameters being kept constant. In particular, when investigating the mass or size ratio dependence of the solute diffusivity, the thermodynamic parameters (temperature T and pressure P) were chosen such that the solvent is a dense liquid, close to its triple point.

Several investigations of diffusion in binary mixtures have been reported in the past. Their objectives, however, differed from ours. Bearman and Jolly [8] studied the mass dependence of the diffusion constant in equimolar mixtures of argon and krypton. Alder and co-workers [9] investigated mass and size dependence of diffusion constants in moderately dense hard-sphere mixtures, their interest being mostly in studying the deviations from Enskog theory due to the appearance of correlated motions in the fluid. A similar study was performed by Toukubo *et al.* [10] on a Lennard-Jones system, but was limited to mass and size ratios of $\frac{1}{2}$ and 2. Finally, the diffusion of an isotope heavier than the solvent molecule was studied by Toxvaerd [11]. In this paper we present a systematic study of small-tracer diffusion in dense fluids using MD simulations.

The paper is organized as follows. Section II describes our model and numerical procedure. The results on the

mass, size, and viscosity dependence of the tracer diffusion coefficient are presented in Sec. III. The paper ends with a brief discussion.

II. MODEL AND NUMERICAL PROCEDURE

Our model "solvent-solute" system was made up to 100 "solvent" (index 1) molecules with 8 "tracer" (index 2) molecules. The interparticle potentials were taken to be a truncated Lennard-Jones interaction:

$$U_{ij}(r) = \epsilon_{ij} f(r/\sigma_{ij}), \quad (3)$$

with additive diameters $\sigma_{ij} = (\sigma_i + \sigma_j)/2$. The truncated Lennard-Jones function $f(x)$ is taken from Ref. [12] and reads

$$f(x) = \begin{cases} 4(x^{-12} - x^{-6}) & \text{for } x < x_c \\ \frac{6}{61\,0009} \left[67 - 48 \frac{x}{x_c} \right]^2 \left[5 - 24 \frac{x}{x_c} \right] & \text{for } x_c < x < x_m \\ 0 & \text{for } x > x_m, \end{cases} \quad (4)$$

where x_c is the inflection point of the LJ potential and $x_m = \frac{67}{48} x_c$. The units of energy, length, and mass were chosen to be, respectively, ϵ_{12} , σ_1 , and m_1 . The corresponding microscopic time scale is $\tau = (m_1 \sigma_1^2 / \epsilon_{12})^{1/2}$. Moreover, we always set the solute-solute interaction energy ϵ_{22} (which in principle would be an irrelevant parameter for an infinitely dilute system) equal to ϵ_{12} . Therefore, the state of our system is fully specified by the choice of five parameters, namely, the mass ratio m_2/m_1 , the size ratio σ_2/σ_1 , the solvent-solvent interaction energy $\epsilon_{11}/\epsilon_{12}$, and two thermodynamic parameters, e.g., the reduced temperature $T^* = k_B T / \epsilon_{12}$ and the reduced density $\rho^* = \rho \sigma_1^3$.

The simulations were carried out at constant volume and temperature using the standard Verlet algorithm and Hoover's thermostatting method [13]. The time step was $h = 0.005\tau$, except in the runs involving very light tracer molecules ($m_2 \leq 0.1m_1$) where a reduction of the time step proved necessary in order to obtain a proper description of the tracer dynamics. Each run consisted typically of 10^4 equilibration steps (starting from a configuration obtained in a previous run) followed by 2×10^4 production steps, during which positions and velocities were recorded for subsequent analysis.

The diffusion constants D_1 and D_2 of the tracer and solvent molecules can be obtained from the mean-square displacement of a tagged particle (Einstein formula),

$$D_i = \lim_{t \rightarrow \infty} \frac{1}{6t} \langle [\mathbf{r}_i(t) - \mathbf{r}_i(0)]^2 \rangle, \quad (5)$$

or equivalently from the integral of its velocity autocorrelation function (Kubo formula),

$$D_i = \frac{1}{3} \int_0^\infty \langle \mathbf{v}_i(t) \cdot \mathbf{v}_i(0) \rangle dt. \quad (6)$$

Both formulas were used to compute the diffusion

coefficients. From the difference between the estimates obtained using Eqs. (5) and (6) and from the scatter between the statistically independent values obtained for the diffusion along the three directions x , y , and z , we estimate the error in our values for D_2 to be about 10%. This unusually large error for a diffusion coefficient is due to the fact that only a small number of tracer molecules contribute to the statistics. In view of this relatively large uncertainty, we did not consider other possible sources of error such as the relatively small system size. Although we are mainly interested in the dynamics of the tracer, the simultaneous calculation of D_1 provides us with a useful reference value. In particular, the solvent viscosity is unknown, so that we cannot directly compare our results for D_2 with Eq. (1). A calculation of the viscosity using either nonequilibrium molecular dynamics or a Green-Kubo formula is, of course, feasible, but would considerably increase the computational effort. We can, however, bypass this difficulty by using Eq. (1) for D_1 [as mentioned in the Introduction, (1) is known to be rather accurate for self-diffusion in simple liquids] to define a "Stokes-Einstein behavior" for D_2 by

$$\frac{D_2}{D_1} = \frac{\sigma_1}{\sigma_2}. \quad (7)$$

As usual, the MD simulation allows one to compute various static quantities such as pair-correlation functions or thermodynamic functions. A static quantity that might be particularly relevant for the understanding of the tracer diffusion (which is a time-dependent process) is the "Einstein frequency distribution" or a tracer molecule defined as follows. For any configuration of the system (characterized by solvent positions \mathbf{R}_i , $i=1, \dots, N_1$ and a tracer position \mathbf{R}_t), we can define the potential $V_t(\mathbf{r})$ created by the solvent molecules on the tracer:

$$V_t(\mathbf{r}) = \sum_{i=1}^{N_1} U_{12}(\mathbf{r} - \mathbf{R}_i). \quad (8)$$

This potential has a matrix of second derivatives evaluated at the tracer position \mathbf{R}_t ,

$$A_{\alpha\beta}(\mathbf{R}_t) = \frac{1}{m_2} \left[\frac{\partial^2 V_t(\mathbf{r})}{\partial r_\alpha \partial r_\beta} \right]_{\mathbf{r}=\mathbf{R}_t}, \quad (9)$$

(the Greek indices refer to Cartesian components, and the m_2^{-1} factor has been introduced so that A has the dimension of a squared frequency), that characterizes the curvature of the potential instantaneously experienced by the tracer particle. If all the three eigenvalues w_1 , w_2 , and w_3 of A are positive, the tracer can be described as being in a "potential well" created by the neighboring solvent molecules. Negative eigenvalues, on the other hand, indicate that the tracer is on a "potential hill." Thus by simply calculating the distribution function of the eigenvalues $w, p(w)$ (which in practice is done by calculating the matrix A and diagonalizing it at each time step, and building a histogram of the resulting eigenvalues), we can easily obtain, e.g., the fraction of time spent by the tracer in the "well" or "hill" configurations, information that is obviously of interest in understanding its diffusion. The

denomination ‘‘Einstein frequency distribution’’ for the normalized distribution $p(w)$ is motivated by the property that its first moment is the square of the Einstein frequency of a tracer particle, defined as usual by

$$\Omega_{E2}^2 = \frac{1}{3m_2} \int d\mathbf{r} \rho_1 g_{12}(r) \nabla^2 U_{12}(r), \quad (10)$$

where ρ_1 is the solvent density and g_{12} the solvent-tracer pair-correlation function. This property stems from the fact that the first moment of $p(w)$ is the average value of the trace of the matrix A , i.e., of $m_2^{-1} \nabla^2 U_{12}(\mathbf{R}_i - \mathbf{R}_i)$. Note that the formulas above refer to the special case of an isolated tracer molecule. When, as is the case in our simulation, the tracer concentration is not vanishingly small, it must be understood that the summation in Eq. (8) also includes the other tracer molecules, and Eq. (10) has to be modified accordingly to include the contribution from the pair-correlation function g_{22} . Finally, we remark that the distribution $p(w)$ is (except for a trivial variable change $w \rightarrow w^{1/2}$) the equivalent at the one-particle level of the normal-mode frequency distribution recently studied in a Lennard-Jones liquid by Seeley and Keyes [14].

As we just mentioned, it is clear that our system, with a tracer concentration of almost 10%, is far from being a dilute solution. The tracer molecules, however, interact in general more weakly with each other and with the solvent than the solvent molecules between themselves. This was indeed the case of the hard-sphere simulations of Eastal and Woolf [15], in which the diffusion constant for a tracer concentration of 12% was found to approach the infinite-dilution value. It is, therefore, reasonable to hope that our results will be close to the ideal, infinite-dilution results. A sensitive check of this expectation is that the solvent and dynamical properties (i.e., its pair-correlation function g_{11} and its diffusion constant D_1) should remain unaffected, and equal to those of the pure solvent at a density n , when some solvent molecules are replaced by tracers. In order to meet this requirements we had in particular to increase slightly the total density as the tracer size was decreased. Tracer-mass variations, which do not affect g_{11} , were also found to have very little effect on D_1 . We also checked that the tracer molecules did not have any tendency to cluster, a behavior that would be indicative of immiscibility between pure tracer and solvent fluids, and can be expected to occur as the mismatch between the two molecules is increased. The formation of clusters was checked for by calculating systematically the number n_{c22} of tracer molecules coordinating another tracer molecule. Except in one case where clustering was observed (see Sec. III C), n_{c22} turned out to be always smaller than 1.

Section III describes the results obtained in three series of runs: in the first series, we vary the tracer size, keeping its mass equal to the solvent mass and all interaction energies equal. Two thermodynamic states of the solvent were studied: a supercritical fluid ($T^*=2.75$, $\rho^*=0.7$) and a state close to the triple point ($T^*=0.75$, $\rho^*=0.85$). As mentioned above, the total density had to be increased as the tracer size was reduced in order to keep g_{11} and D_1

constant. In the second series of runs, we vary the tracer’s mass for several fixed size ratios, the interaction energies being still identical. Here only the state of the solvent close to the triple point was considered. Finally, a third series of runs explores, for several tracer sizes, the dependence of D_1 on the solvent’s viscosity, for equal masses, a fixed temperature $T^*=T/\varepsilon_{12}=0.75$, and a fixed density $\rho^*=0.85$. The solvent viscosity was increased by increasing the solvent-solvent interaction energy ε_{11} , so that the solvent effectively becomes a supercooled Lennard-Jones liquid with a ‘‘solvent reduced temperature,’’ $T_1^*=T/\varepsilon_{11}$, smaller than 0.75.

III. RESULTS

A. Size dependence

Our findings for the size dependence of the tracer diffusion for a mass ratio of 1 are summarized in Figs. 1(a) and 1(b) and Tables I and II. In order to facilitate the comparison with the Stokes-Einstein relation [Eq. (7)], we have plotted in these figures the ratio D_2/D_1 versus σ_1/σ_2 . The behavior of D_2 is rather similar for the two temperatures investigated: in both cases, D_2 first increases as the tracer size decreases, then levels off at a size-independent value. This leveling off takes place for size ratios σ_1/σ_2 between 5 and 10. For $\sigma_2 \leq 0.1\sigma_1$, the tracer behaves essentially as a pointlike particle in the external potential created by the solvent molecules, and its size becomes irrelevant. The most noticeable difference between the two temperatures is in the initial increase of D_2 . While for $T^*=2.75$, this initial increase can be described by Eq. (7), a strong positive deviation from this Stokes-Einstein behavior occurs at $T^*=0.75$. Such a positive deviation is compatible with the experimental observations that the Stokes-Einstein relation underestimates the tracer diffusion coefficient when solvent viscosity is high (note that σ_1/σ_2 is usually smaller than 10 in the experiments). This effect can be described using Eq. (2) or equivalently and *ad hoc* ‘‘viscosity-dependent radius’’ which increases with solvent viscosity [16].

Figure 2 presents the Einstein frequency distributions

TABLE I. Diffusion coefficient D_2 of the tracer molecules for various size ratios σ_2/σ_1 . The thermodynamic state of the pure solvent is $T^*=0.75$, $\rho^*=0.85$. The total density is increased as the tracer size is reduced.

m_2/m_1	σ_2/σ_1	ρ^*	D_2	D_1
1.0	1.0	0.850	0.027	0.024
1.0	0.90	0.868	0.029	0.025
1.0	0.70	0.890	0.046	0.025
1.0	0.50	0.900	0.079	0.026
1.0	0.35	0.900	0.13	0.026
1.0	0.20	0.910	0.21	0.028
1.0	0.15	0.910	0.25	0.027
1.0	0.10	0.920	0.33	0.025
1.0	0.075	0.920	0.36	0.027
1.0	0.06	0.920	0.355	0.028
1.0	0.05	0.920	0.39	0.024

TABLE II. Diffusion coefficient D_2 of the tracer molecules for various size ratios σ_2/σ_1 . The thermodynamic state of the pure solvent is $T^*=2.75$, $\rho^*=0.7$.

m_2/m_1	σ_2/σ_1	ρ^*	D_2	D_1
1.0	1.00	0.700	0.27	0.25
1.0	0.70	0.740	0.38	0.24
1.0	0.30	0.765	0.63	0.24
1.0	0.15	0.768	1.01	0.24
1.0	0.10	0.770	1.32	0.24
1.0	0.08	0.771	1.28	0.24
1.0	0.05	0.775	1.45	0.24

for a small tracer ($\sigma_2=0.1\sigma_1$) and a larger one ($\sigma_2=0.9\sigma_1$). A trivial difference between the two curves is, of course, the typical magnitude of the eigenvalues w , which is much smaller for the small tracer, this difference being obviously due to the weaker interaction potential. A more interesting feature is the fact that while for the bigger tracer only 1% of the eigenvalues are negative, this proportion reaches 31% for the smaller one. The big tracer is therefore almost always in the bottom of a potential well created by its neighbors, so that its motion necessarily involves a collective motion of these neigh-

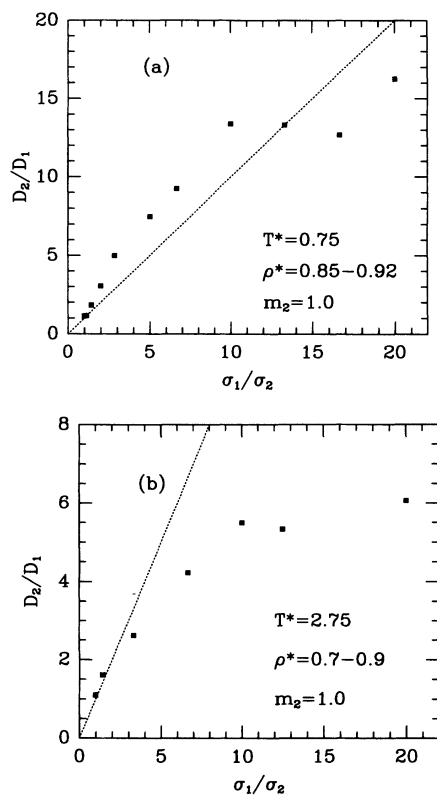


FIG. 1. (a) The ratio of tracer over solvent diffusion coefficients D_2/D_1 as a function of the inverse size ratio, for equal masses. The thermodynamic state of the pure solvent is $T^*=0.75$, $\rho^*=0.85$; the density is increased from 0.85 to 0.92 as the tracer size is decreased. The dashed line corresponds to the Stokes-Einstein behavior [Eq. (7)]. (b) Same as (a), but for a supercritical solvent ($T^*=2.75$, $\rho^*=0.7$).

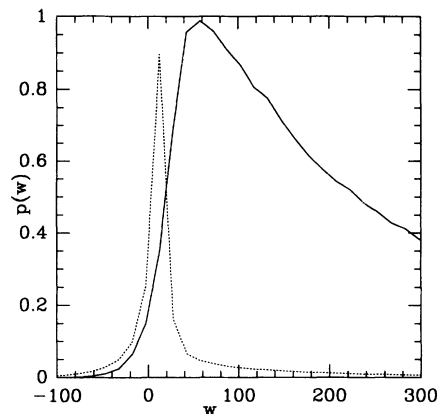


FIG. 2. Einstein frequency distribution of the solute molecules. Solid curve, $\sigma_2=0.9\sigma_1$; dashed curve, $\sigma_2=0.1\sigma_1$. The thermodynamic state of the solvent is $T^*=0.75$, $\rho^*=0.85$; the mass ratio is 1.

bors. On the contrary, the small particle spends a large fraction of time hopping over potential barriers, a behavior that is consistent with the “point-particle” picture we inferred from the size dependence of D_2 .

B. Mass dependence

The dependence of D_2 on m_2 has been investigated for diameter ratios of 1, 0.5, and 0.1, for a solvent close to its triple point ($T^*=0.75$, $0.85 \leq \rho^2 \leq 0.92$), all interaction energies being kept equal. The prediction from the Stokes-Einstein equation (1) is that D_2 should be independent of m_2/m_1 . This prediction is borne out for $\sigma_2/\sigma_1=1$ (isotope diffusion): in this case, we found that D_2 is essentially independent of m_2/m_1 in the range $0.05m_1 \leq m_2 \leq m_1$. The situation is quite different for the two other diameter ratios, as illustrated in Figs. 3(a) and 3(b) and Tables III and IV. In both case, D_2 starts to increase rapidly with decreasing m_2 when m_2/m_1 becomes smaller than about 0.5. Once again, we observe that using the Stokes-Einstein relation would yield an underestimate of D_2 .

C. Solvent-viscosity dependence

In order to simulate an increase in solvent viscosity at fixed temperature, we increased the solvent-solvent in-

TABLE III. Diffusion coefficient D_2 as a function of mass ratio m_2/m_1 for a size ratio $\sigma_2/\sigma_1=0.5$. The thermodynamic state is $T^*=0.75$, $\rho^*=0.9$.

σ_2/σ_1	m_2/m_1	D_2	D_1
0.5	1.00	0.08	0.026
0.5	0.70	0.08	0.026
0.5	0.50	0.09	0.026
0.5	0.40	0.10	0.026
0.5	0.30	0.09	0.026
0.5	0.10	0.13	0.026
0.5	0.05	0.14	0.026

TABLE IV. Diffusion coefficient D_2 as a function of mass ratio m_2/m_1 for a size ratio $\sigma_2/\sigma_1=0.1$. The thermodynamic state is $T^*=0.75$, $\rho^*=0.92$. The number density is slightly higher than that in Table III because the tracer size is smaller.

σ_2/σ_1	m_2/m_1	D_2	D_1
0.1	1.00	0.33	0.025
0.1	0.70	0.37	0.025
0.1	0.50	0.35	0.025
0.1	0.40	0.44	0.025
0.1	0.25	0.54	0.025
0.1	0.10	0.70	0.025
0.1	0.05	0.78	0.025

teraction energy, all other parameters being kept fixed. This was done for diameter ratios of 0.5 and 0.1, at $T^*=0.75$. Before commenting on the results, we briefly point out some difficulties associated with the use of a supercooled solvent: It is well known that a one-component supercooled Lennard-Jones liquid will crystallize unless a high quenching rate is applied [17]. The use of a high quenching rate on the sluggish supercooled solvent implies that the system cannot be well equilibrated. Moreover, crystalline nucleation is always possible, and we had in fact to discard several runs because of its

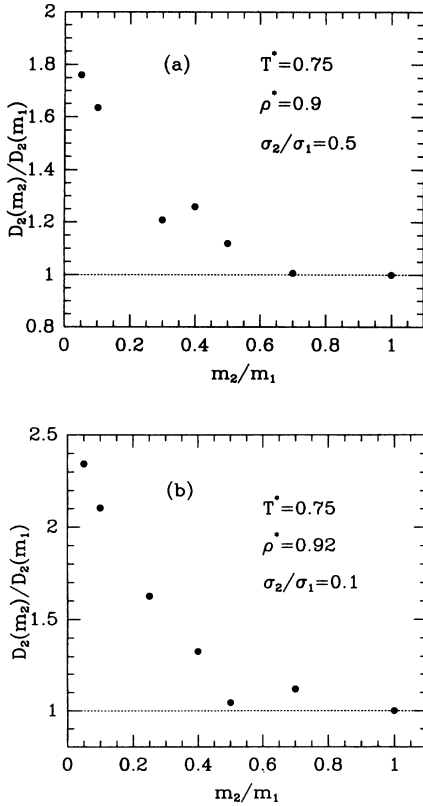


FIG. 3. (a) Tracer diffusion coefficient as a function of mass ratio for a size ratio $\sigma_2/\sigma_1=0.5$. The temperature and density are $T^*=0.75$, $\rho^*=0.90$. The dashed line corresponds to the Stokes-Einstein behavior [Eq. (7)]. (b) Same as (a), but for a smaller size ratio $\sigma_2/\sigma_1=0.1$. The temperature and density are $T^*=0.75$, $\rho^*=0.92$.

TABLE V. Diffusion coefficients D_1 and D_2 at various solvent-solvent interaction energies ϵ_{11} . The temperature and density are $T^*=0.75$, $\rho^*=0.9$ and the size ratio is 0.5.

m_2/m_1	σ_2/σ_1	T^*/ϵ_{11}	D_1	D_2
1.0	0.5	0.95	0.033	0.100
1.0	0.5	0.85	0.031	0.093
1.0	0.5	0.75	0.026	0.079
1.0	0.5	0.65	0.021	0.083
1.0	0.5	0.55	0.018	0.069
1.0	0.5	0.50	0.014	0.071
1.0	0.5	0.45	0.011	0.070

occurrence. Another worrisome aspect is the possibility of phase separation between tracer and solvent, which is expected to be enhanced for large $\epsilon_{11}/\epsilon_{12}$ ratios. This phase separation results in a clustering of the tracer molecules, and runs where such a clustering was detected had to be discarded.

As a consequence of these difficulties, only a limited range of ϵ_{11} ($0.4 \leq T^*/\epsilon_{11} \leq 0.95$) values was investigated. This corresponds to a decrease in D_1 (and therefore, if we assume that the SE relation is valid for self-diffusion, an increase in solvent viscosity) by a factor of

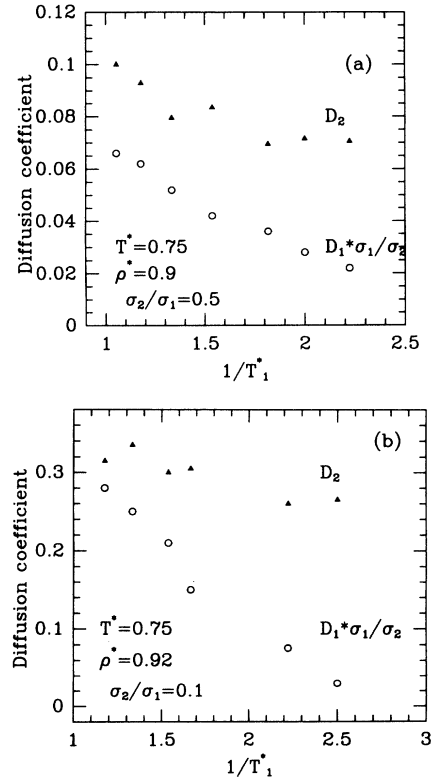


FIG. 4. (a) Solute (triangles) and solvent (circles) diffusion coefficient vs inverse “reduced solvent temperature” ϵ_{11}/T^* , for a size ratio $\sigma_2/\sigma_1=0.5$. The system temperature is fixed at $T^*=0.75$ and the total density is 0.9; the masses are equal. D_1 has been multiplied by σ_1/σ_2 in order to facilitate the comparison with Eq. (7). (b) Same as (a), but for a smaller size ratio $\sigma_2/\sigma_1=0.1$. The density is therefore slightly higher: $\rho^*=0.92$.

TABLE VI. Same as Table V but for a size ratio of 0.1. The temperature and density are $T^*=0.75$, $\rho^*=0.92$.

m_2/m_1	σ_2/σ_1	T^*/ϵ_{11}	D_1	D_2
1.0	0.1	0.85	0.028	0.31
1.0	0.1	0.75	0.025	0.33
1.0	0.1	0.65	0.021	0.30
1.0	0.1	0.60	0.015	0.30
1.0	0.1	0.45	0.007	0.26
1.0	0.1	0.40	0.003	0.26

about 10. The density was kept constant, $\rho^*=0.9$ for $\sigma_2/\sigma_1=0.5$ and $\rho^*=0.92$ for $\sigma_2/\sigma_1=0.1$. The results are presented in Figs. 4(a) and 4(b) and Tables V and VI. For $\sigma_2/\sigma_1=0.5$, D_2 first decreases as ϵ_{11}/T^* increases, then seems to level off for $\epsilon_{11}/T^* \geq 1.5$, indicating a decoupling between solvent and tracer motions. For $\sigma_2/\sigma_1=0.1$, the dependence of D_2 on ϵ_{11}/T^* is apparently very weak, showing the tracer dynamics is completely independent of the solvent dynamics in the range of viscosities we considered.

IV. DISCUSSION AND CONCLUSIONS

The results presented in Sec. III all display some kind of decoupling phenomenon occurring when the solvent and the tracer become increasingly dissimilar. This decoupling results in strong positive deviations from the SE behavior, in qualitative agreement with experimental observations. An obvious theoretical framework for the interpretation of our results is the Mori-Zwanzig projection-operator formalism combined with mode-coupling approximations for the memory functions [3]. A simplified version was recently proposed by Gaskell and co-workers [18] and seems to account well for self-diffusion in simple liquids. In this type of theory the inverse of the diffusion coefficient of a tagged particle is usually written as a sum of two terms, $D_2^{-1} = D_B^{-1} + D_{MC}^{-1}$. The first term accounts for decorrelated binary collisions between the tagged particle and the other particles in the fluid that occur on short time scales. The second one is a "mode-coupling" term, which describes the coupling of the tagged particle motion to the slow hydrodynamic modes of the fluid. We expect

that the various decouplings we observe correspond to the fact that as the tracer becomes much smaller or much lighter than the solvent, the mode-coupling term becomes small compared to the binary collision term. The tracer can escape the cage created by its neighbors by hopping over potential barriers, without needing a global rearrangement of its environment, and the mode-coupling term becomes unimportant. Since only the binary term depends on the mass of the tracer, while only the mode-coupling term depends on the solvent viscosity, this interpretation is obviously consistent with the results of Secs. III B and III C. A more quantitative analysis, however, will obviously be necessary and is presently in progress.

In this paper we have presented a detailed investigation of the diffusion of a small Lennard-Jones tracer in a solvent of similar molecules. This work was motivated by the existence of numerous experimental results on tracer diffusion exhibiting strong deviations from Stokes-Einstein behavior. We did not, however, attempt a comparison with any specific experiment, but rather chose to study a simple model in order to assess the separate influence of the different parameters characterizing the solvent-tracer diffusion couple. We expect that theories capable of reproducing our results for such a model system could be usefully extended to experimental situations. In the simulations we observed deviations similar to those found in experiments when the tracer size, the tracer mass, and the solvent viscosity were varied. The dependence of the tracer diffusivity on these various parameters is quite complex, with crossovers between regions in which the solvent dynamics strongly influences the tracer diffusion and regions in which the tracer behaves as a particle diffusing in a static external potential. In view of this complexity, it seems theoretically difficult to justify the use of a simple empirical formula relating tracer diffusivity and solvent viscosity, such as Eq. (2).

ACKNOWLEDGMENTS

We wish to thank Professor J. P. Hansen for useful discussions. Laboratoire de Physique is "Unité Recherche 1325 Associée au CNRS."

*Present address: International Centre for Theoretical Physics, Condensed Matter Group, P.O. Box 586, 34100 Trieste, Italy.

[1] G. Phillies, *J. Phys. Chem.* **85**, 2838 (1981).

[2] D. Forster, *Hydrodynamic Fluctuations, Broken Symmetry, and Correlation Functions* (Benjamin, Reading, MA, 1975).

[3] J.-P. Hansen and I. R. McDonald, *Theory of Simple Liquids* (Academic, London, 1986).

[4] T. G. Hiss and E. L. Cussler, *AIChE J.* **19**, 698 (1973).

[5] H. J. V. Tyrrell and K. R. Harris, *Diffusion in Liquids: A Theoretical and Experimental Study* (Butterworths, London, 1984).

[6] G. L. Pollack and J. Enyeart, *Phys. Rev. A* **31**, 980 (1985).

[7] G. L. Pollack, R. P. Kennan, J. F. Himm, and D. R. Stump, *J. Chem. Phys.* **92**, 625 (1990).

[8] R. J. Bearman and D. L. Jolly, *Mol. Phys.* **44**, 665 (1981).

[9] B. J. Alder, W. E. Alley, and J. H. Dymond, *J. Chem. Phys.* **61**, 1415 (1974).

[10] K. Toukubo, K. Nakanishi, and N. Watanabe, *J. Chem. Phys.* **67**, 4162 (1977).

[11] S. Toxvaerd, *Mol. Phys.* **56**, 1017 (1985).

[12] J.-P. Ryckaert, A. Bellemans, G. Ciccoti, and G. V. Paolini, *Phys. Rev. A* **39**, 259 (1989).

[13] M. Allen and D. Tildesley, *Computer Simulation of Liquids* (Oxford University Press, Oxford, England, 1987).

- [14] G. Seeley and T. Keyes, *J. Chem. Phys.* **91**, 5581 (1989).
- [15] A. J. Easteal and L. A. Woolf, *Chem. Phys. Lett.* **167**, 329 (1990).
- [16] D. C. Champeney and F. Ould-Kaddour, *Mol. Phys.* **52**, 509 (1984).
- [17] F. Yonezawa, S. Nosé, and S. Sakamoto, *Z. Phys. Chem.* **156**, 77 (1988).
- [18] U. Balucani, R. Vallauri, T. Gaskell, and S. F. Duffy, *J. Phys. Condens. Matter* **2**, 5015 (1990).